

University of Groningen

Extracellular Proteome and Citrullinome of the Oral Pathogen *Porphyromonas gingivalis*

Stobernack, Tim; Glasner, Corinna; Junker, Sabryna; Gabarrini, Giorgio; de Smit, Menke; de Jong, Anne; Otto, Andreas; Becher, Doerte; van Winkelhoff, Arie Jan; van Dijk, Jan Maarten

Published in:
Journal of Proteome Research

DOI:
[10.1021/acs.jproteome.6b00634](https://doi.org/10.1021/acs.jproteome.6b00634)

IMPORTANT NOTE: You are advised to consult the publisher's version (publisher's PDF) if you wish to cite from it. Please check the document version below.

Document Version
Publisher's PDF, also known as Version of record

Publication date:
2016

[Link to publication in University of Groningen/UMCG research database](#)

Citation for published version (APA):

Stobernack, T., Glasner, C., Junker, S., Gabarrini, G., de Smit, M., de Jong, A., Otto, A., Becher, D., van Winkelhoff, A. J., & van Dijk, J. M. (2016). Extracellular Proteome and Citrullinome of the Oral Pathogen *Porphyromonas gingivalis*. *Journal of Proteome Research*, 15(12), 4532-4543.
<https://doi.org/10.1021/acs.jproteome.6b00634>

Copyright

Other than for strictly personal use, it is not permitted to download or to forward/distribute the text or part of it without the consent of the author(s) and/or copyright holder(s), unless the work is under an open content license (like Creative Commons).

The publication may also be distributed here under the terms of Article 25fa of the Dutch Copyright Act, indicated by the "Taverne" license. More information can be found on the University of Groningen website: <https://www.rug.nl/library/open-access/self-archiving-pure/taverne-amendment>.

Take-down policy

If you believe that this document breaches copyright please contact us providing details, and we will remove access to the work immediately and investigate your claim.

Downloaded from the University of Groningen/UMCG research database (Pure): <http://www.rug.nl/research/portal>. For technical reasons the number of authors shown on this cover page is limited to 10 maximum.

Extracellular Proteome and Citrullinome of the Oral Pathogen *Porphyromonas gingivalis*

Tim Stoernack,^{†,‡} Corinna Glasner,^{†,‡} Sabryna Junker,[‡] Giorgio Gabarrini,^{†,§} Menke de Smit,[§] Anne de Jong,^{||} Andreas Otto,[‡] Dörte Becher,[‡] Arie Jan van Winkelhoff,^{†,§} and Jan Maarten van Dijk^{*,†}

[†]Department of Medical Microbiology, University of Groningen, University Medical Center Groningen, Groningen 9700 RB, The Netherlands

[‡]Institute for Microbiology, Ernst-Moritz-Arndt-University Greifswald, Greifswald 17489, Germany

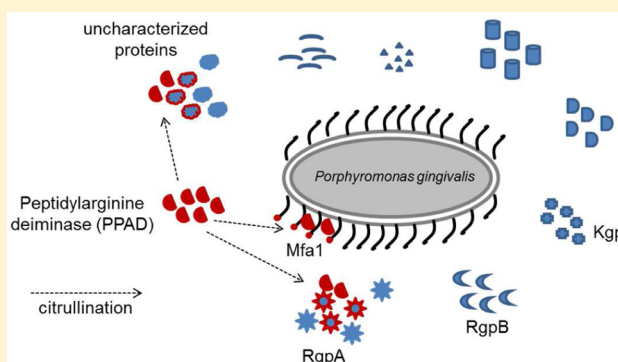
[§]Center for Dentistry and Oral Hygiene, Department of Periodontology, University of Groningen, University Medical Center Groningen, Groningen 9700 RB, The Netherlands

^{||}Department of Molecular Genetics, University of Groningen, Groningen 9700 AB, The Netherlands

S Supporting Information

ABSTRACT: *Porphyromonas gingivalis* is an oral pathogen associated with the inflammatory disease periodontitis. Periodontitis and *P. gingivalis* have been associated with rheumatoid arthritis. One of the hallmarks of rheumatoid arthritis is the loss of tolerance against citrullinated proteins. Citrullination is a post-translational modification of arginine residues, leading to a change in structure and function of the respective protein. This modification, which is catalyzed by peptidylarginine deiminases (PADs), plays a role in several physiological processes in the human body. Interestingly, *P. gingivalis* secretes a citrullinating enzyme, known as *P. gingivalis* PAD (PPAD), which targets bacterial and human proteins. Because the extent of *P. gingivalis* protein citrullination by PPAD was not yet known, the present study was aimed at identifying the extracellular proteome and citrullinome of *P. gingivalis*. To this end, extracellular proteins of two reference strains, two PPAD-deficient mutants, and three clinical isolates of *P. gingivalis* were analyzed by mass spectrometry. The results uncovered substantial heterogeneity in the extracellular proteome and citrullinome of *P. gingivalis*, especially in relation to the extracellular detection of typical cytoplasmic proteins. In contrast, the major virulence factors of *P. gingivalis* were identified in all investigated isolates, although their citrullination was shown to vary. This may be related to post-translational processing of the PPAD enzyme. Altogether, our findings focus attention on the possible roles of 6 to 25 potentially citrullinated proteins, especially the gingipain RgpA, in periodontitis and rheumatoid arthritis.

KEYWORDS: *Porphyromonas gingivalis*, protein sorting, exoproteome, citrullination, peptidylarginine deiminase



INTRODUCTION

Periodontitis is an inflammatory disease affecting the soft and hard tissues surrounding the teeth. It is primarily caused by bacterial deposits organized in a subgingival biofilm. Severe periodontitis has a prevalence of 10–15% in the general adult population and is the major cause for tooth loss over the age of 35.^{1,2} Subgingival carriage of *Porphyromonas gingivalis* has been implicated in the development of periodontitis in susceptible hosts.^{3–6} Interestingly, *P. gingivalis* and periodontitis have both been associated with systemic diseases like rheumatoid arthritis (RA).^{2,7–9} RA is a chronic inflammation of synovial joints with a prevalence of 0.5 to 1.0% in the general population. A specific feature of RA development is the loss of tolerance to citrullinated proteins. This correlates with the formation of anticitrullinated protein antibodies (ACPAs) that seem to trigger a preclinical state of the disease^{2,8,10,11} and are associated

with a poorer disease outcome or increased joint damage and low remission rates.¹²

Citrullination is a post-translational protein modification where L-arginine is enzymatically converted to L-citrulline, which causes changes in the charge and structure of the respective target proteins.¹³ In the human body, citrullination occurs during cell apoptosis, and it is an important factor in skin keratinization, insulation of neurons, general development of the central nervous system, and various gene regulatory mechanisms.^{13–16} Citrullination is catalyzed by peptidylarginine deiminases (PADs), of which five isotypes have been identified in humans. An analogous enzyme is found in *P. gingivalis*. To date, *P. gingivalis* is the only bacterium known to produce a PAD enzyme.^{17–19} Studies have shown that the *P. gingivalis*

Received: July 8, 2016

Published: October 7, 2016

PAD (PPAD) citrullinates not only bacterial but also human proteins (e.g., α -enolase and vimentin). This mechanism of human protein citrullination by PPAD may be a connection between periodontitis and RA.^{11,13}

P. gingivalis is a Gram-negative bacterium. Accordingly, it has a cell envelope consisting of two distinct membranes, the inner membrane and the outer membrane, which enclose the periplasm. Thus at least five subproteomes can be distinguished, specifically the cytoplasmic, inner membrane, periplasmic, outer membrane, and exoproteome. The outer membrane acts as a permeation barrier that serves in the cellular retention of periplasmic proteins. Many virulence factors of Gram-negative bacteria are located in/on the outer membrane or are secreted. Important proteinaceous virulence factors of *P. gingivalis* are fimbriae and gingipains. The fimbriae are appendages that enable this pathogen to attach to other bacteria or to host cells, which is important in biofilm formation. Gingipains are cysteine proteinases and account for 85% of the total proteolytic activity of *P. gingivalis*.^{4,20}

Notably, the secreted PPAD can be regarded as another virulence factor that may impact the host's immune system by increasing the level of citrullinated proteins. This could lead to a loss of tolerance against citrullinated proteins and the subsequent development of RA, which raises the question to what extent PPAD citrullinates the proteins that *P. gingivalis* secretes into its extracellular milieu. Conceivably, such citrullinated bacterial proteins could contribute to the overall citrullination burden in the human host. Several previous studies investigated the overall proteome of *P. gingivalis* exposed to different conditions.^{21–27} However, to date, very little is known about the exoproteome composition of especially clinical isolates of *P. gingivalis* and the extent to which the respective proteins are citrullinated. Therefore, the aim of this study was to define the exoproteome of *P. gingivalis* and to investigate the possible citrullination of the identified proteins by mass spectrometry (MS). To this end, different *P. gingivalis* reference strains including two PPAD mutants as well as clinical isolates were investigated. This allowed a definition of the core and variable exoproteomes. Importantly, a number of citrullinated exoproteins of *P. gingivalis* were identified, which are collectively referred to as the *P. gingivalis* “citrullinome”.

MATERIAL AND METHODS

P. gingivalis Isolates Used in This Study

The *P. gingivalis* reference strains ATCC 33277 and W83 as well as two respective PPAD-deficient mutants¹⁸ were used. Furthermore, three previously described clinical isolates were analyzed,¹⁷ which had been obtained from a patient with severe periodontitis without RA (20658), a patient with moderate periodontitis and RA (MDS16), and a patient with severe periodontitis and RA (MDS45).

Growth Conditions

Bacteria were grown anaerobically either on Blood Agar Base No. 2 (BA2) plates or in brain heart infusion (BHI) broth (Oxoid, Basingstoke, U.K.) that contained 5% (w/v) L-cysteine, 5 mg/L hemin, and 1 mg/L menadione. Prior to inoculation, the BHI broth was prereduced for 3 days in an anaerobic chamber.

To start liquid cultures, 5 day old colonies from BA2 plates were inoculated anaerobically into serum bottles with a rubber septum in the cap that contained 30 mL of BHI broth. The colonies were then dispersed in the BHI broth using a syringe

with a 21G needle. Lastly, the bottles were tightly closed and anaerobically incubated at 37 °C. For proteome analyses, culture samples were collected in the stationary phase after 24 to 32 h of growth using a syringe with a 21G needle.

Species Verification

P. gingivalis colonies grown on BA2 plates were verified by matrix-assisted laser desorption/ionization-time-of-flight (MALDI-TOF) MS using a MALDI Biotyper (Bruker Corporation, Billerica, MA). In brief, one single colony was spotted twice on the MALDI target of a mass spectrometer. Next, 1 μ L of buffer (containing formaldehyde) was added to each spot. After ~25 min of incubation, 1 μ L of matrix material (α -cyano-4-hydroxycinnamic acid, Sigma-Aldrich, St. Louis, MO) was added to each spot and MS spectra were recorded. A minimum score value of 2.0 was used as a criterion for *P. gingivalis* identification.²⁸

Preparation of Exoproteome Samples

To analyze the exoproteome of *P. gingivalis*, cells were grown in triplicates in liquid culture until early stationary phase (approximately 24–32 h of growth). Two mL of culture was centrifuged for 10 min at 8000g and 4 °C. 1.2 mL of the supernatant was added to 0.3 mL of 50% trichloroacetic acid (TCA, Sigma-Aldrich), mixed thoroughly, and stored on ice at 4 °C overnight for precipitation of proteins. To collect the precipitated proteins, the sample was centrifuged for 20 min at 13 200g and 4 °C. After one washing step with 500 μ L of ice-cold pure acetone, the pellet was collected again by centrifugation for 10 min at 14 000 rpm and 4 °C. The acetone was removed and the protein pellet was dried at room temperature or 60 °C and stored at –20 °C until further use.

LDS-PAGE

Lithium dodecyl sulfate (LDS) PAGE was performed using 10% NuPAGE gels (Invitrogen, Carlsbad, CA). Cells were resuspended in LDS buffer (Life Technologies) and disrupted by bead-beating with 0.1 μ m glass beads (Biospec Products, Bartlesville, OK) using a Precellys24 (Bertin Technologies, Montigny-le-Bretonneux, France), and exoproteins were precipitated from the growth medium with 10% TCA (4 °C, overnight). Protein samples were incubated for 10 min at 95 °C, separated by LDS-PAGE, and stained with SimplyBlue SafeStain (Life Technologies, Carlsbad, CA).

Sample Preparation for Mass Spectrometry

Dried exoproteome pellets were first digested following an in-solution trypsin digestion procedure. The whole-protein pellets were resuspended in 100 μ L of 50 mM ammonium bicarbonate buffer (Fluka, Buchs, Switzerland). The samples were reduced by the addition of 2 μ L of 500 mM DTT and incubation for 45 min at 60 °C. Subsequently, the samples were alkylated by the addition of 2 μ L of 500 mM iodoacetamide (IAA, Sigma-Aldrich) and incubated in the dark for 15 min at room temperature. Trypsin (80 ng; Promega, Madison, WI) was added, and samples were incubated overnight at 37 °C under continuous shaking at 250 rpm. The trypsin digestion was stopped by the addition of 0.1% trifluoroacetic acid (TFA, Sigma-Aldrich) and incubation at 37 °C for 45 min.

To purify in-solution digested peptides, a ZipTip (Millipore, Billerica, MA) filtration procedure was implemented as described by Dreisbach et al.²⁹ In brief, after wetting and equilibrating a ZipTip pipet tip, the peptides were bound to C-18 material. A subsequent washing step with 0.1% acetic acid was followed by a final elution with 60% acetonitrile and 0.1%

acetic acid. The samples were dried at room temperature in a Concentrator Plus Speed Vac (Eppendorf, Hamburg, Germany) using the V-AQ program, and the resulting peptide pellets were stored at 4 °C until further use.

Mass Spectrometry Analysis

Purified peptides were analyzed by reversed-phase liquid chromatography (LC) electrospray ionization (ESI) MS/MS using an LTQ Orbitrap XL (Thermo Fisher Scientific, Waltham, MA) as described by Bonn et al.³⁰ In brief, in-house self-packed nano-LC columns (20 cm) were used to perform LC with an EASY-nLC II system (Thermo Fisher Scientific). The peptides were loaded with buffer A (0.1% acetic acid (v/v)) and subsequently eluted by a binary gradient of buffer A and B (0.1% acetic acid (v/v), 99.9% acetonitrile) over a period of 80 min. After injection into the MS, a full scan was recorded in the Orbitrap with a resolution of 30 000. The five most abundant precursor ions were consecutively isolated in the LTQ XL and fragmented via collision-induced dissociation (CID). Unassigned charge states as well as singly charged ions were rejected, and the lock mass option was enabled.

Database searching was done with Sorcerer-SEQUEST 4 (Sage-N Research, Milpitas, CA). After extraction from the raw files, *.dta files were searched with Sequest against a target-decoy database with a set of common laboratory contaminants. A nonredundant database for the respective peptide/protein search was created from the published genome sequences of the W83, ATCC 33277, and TDC60, strains which were downloaded from Uniprot (<http://www.uniprot.org>) on 10/21/2014 (Supplementary FASTA file). The created database contained a total number of 12 254 proteins. Protein sequences that differed in only one amino acid were included in this database. Of note, some poorly conserved proteins of the clinical isolates will be missing from the database because their genome sequences have not been determined. Database search was based on a strict trypsin digestion with two missed cleavages permitted. No fixed modifications were considered. Oxidation of methionine, carbamidomethylation of cysteine, and citrullination of arginine were considered as variable modifications. The mass tolerance for precursor ions was set to 10 ppm and the mass tolerance for fragment ions was set to 0.5 Da. Validation of MS/MS-based peptide and protein identification was performed with Scaffold v.4.4.1.1 (Proteome Software, Portland, OR). Peptide identifications were accepted if they exceeded the following specific database search engine thresholds. SEQUEST identifications required at least deltaCn scores of greater than 0.1 and XCorr scores of greater than 2.2, 3.3, and 3.75 for doubly, triply, and all higher charged peptides, respectively. Protein identifications were accepted if at least two identified peptides were detected with the above-mentioned filter criteria in two out of three biological replicates. With these filter parameters, no false-positive hits were obtained, as was verified by a search against a concatenated target-pseudoreversed decoy database. However, it should be noted that these filter parameters can potentially lead to false-negative hits, especially in the case of low-abundant proteins. Thus if a protein is not identified, this does not necessarily mean that it is not present at all.

Protein data were exported from Scaffold and further curated in Microsoft Excel 2010 before further analysis. The MS proteomics data have been deposited to the ProteomeXchange Consortium via the PRIDE partner repository³¹ with the data set identifier PXD003444.

Quantitative values of protein abundances were obtained by summing up all spectra associated with a specific protein within a sample, which also includes those spectra that are shared with other proteins. To allow comparisons, we normalized spectral counts by applying a scaling factor for each sample to each protein by adjusting the values to normalized spectral counts. Of note, some proteins are easier to detect than others, which may affect the comparison of abundance levels of different proteins.

Citrullination of proteins was detected by a mass shift of 1 Da in arginine-containing peptides. To exclude false-positive identifications, peptides containing asparagine or glutamine were excluded from this analysis because it is not possible to distinguish between citrullination of arginine and deamidation of asparagine or glutamine. The spectra and fragmentation tables of six identified citrullinated proteins are shown in Supplementary Figure S6.

Statistical Analyses

Statistical analyses of the relative exoprotein abundances were performed as follows. Replicate values of the normalized total spectral counts were imported into GraphPad Prism 6 (GraphPad Software, La Jolla, CA). A Two-Way ANOVA Turkey's multiple comparison test was performed, where the mean exoprotein abundance values of every bacterial isolate were compared with each other within every single exoprotein row in the respective heatmap. This led to the detection of simple effects within each exoprotein row. The total number of significant differences within the 20 most abundant and within the 50 least abundant exoproteins was used as a measure of heterogeneity in the respective fractions of the bacterial exoproteomes.

Bioinformatic Analyses

Protein localization predictions were performed using the following algorithms: LipoP (version 1.0),³² Lipo (version 1.0),³³ TMHMM (version 2.0),^{34,35} Phobius (version 1.0),³⁶ SignalP (version 4.1),³⁷ Predisi (version 1.0),³⁸ SecretomeP (version 2.0),³⁹ PsortB (version 3.0),⁴⁰ and ClubSub (version 2.18.3).⁴¹ Furthermore, manual curation based on *Bacteroidetes/Porphyromonas*-specific domain identification⁵⁴ was done for proteins with unclear localization predictions.

For visualization of protein functions, the gene ontology (GO) terms of the present protein data set were imported into the REVIGO software.⁴²

Biological and Chemical Safety

P. gingivalis is a biosafety level 2 (BSL-2) microbiological agent and was accordingly handled following appropriate safety procedures. All experiments involving live *P. gingivalis* bacteria and chemical manipulations of *P. gingivalis* protein extracts were performed under appropriate containment conditions, and protective gloves were worn. All chemicals and reagents used in this study were handled according to the local guidelines for safe usage and protection of the environment.

RESULTS

Exoproteomes of *P. gingivalis* Reference Strains and Clinical Isolates

A total of seven *P. gingivalis* reference strains and clinical isolates were examined in the present study. Growth experiments in BHI broth revealed some differences in growth rates and maximal optical density (OD) at 600 nm, especially between the reference strains and the clinical isolates. As shown

in Supplementary Figure S1, the reference strains displayed higher growth rates while reaching lower maximum ODs. Because only a few proteins were found to be secreted by exponentially growing cells compared with stationary phase cells (Supplementary Figure S2), exoproteome analyses were only performed on early stationary phase samples. Furthermore, as shown by LDS-PAGE (Figure S2), the different isolates revealed different protein banding patterns, suggesting isolate-specific variations in their exoproteome composition. On the basis of these observations, the exoproteome fractions of the different *P. gingivalis* isolates were further analyzed by the gel-free proteomics approach LC-ESI-MS/MS. A total number of 257 proteins was identified in the combined exoproteome of the seven different isolates (Supplementary Table S1). The total numbers of proteins identified per isolate ranged from 124 to 202 proteins (Supplementary Figure S3A). Remarkably, 202 extracellular proteins were identified for the MDS45 isolate, while for all other isolates between 124 and 147 extracellular proteins were identified.

Figure 1 illustrates the overlaps and differences in the exoproteomes of the investigated isolates. While the two

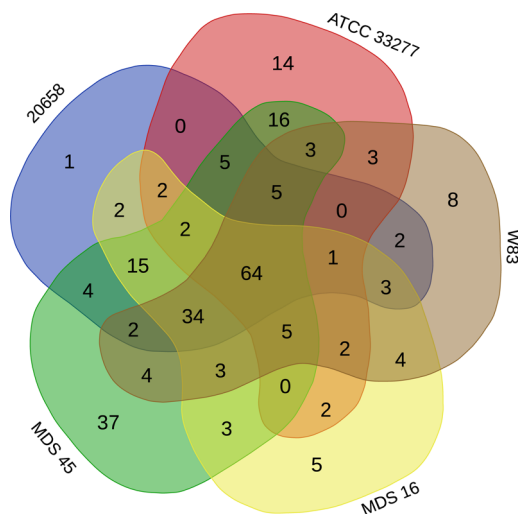


Figure 1. Differential detection of proteins in the exoproteomes of the *P. gingivalis* isolates. Venn diagram giving an overview of the numbers of consistently or uniquely identified proteins in the two reference strains W83 and ATCC 33277 and the three clinical isolates 20658, MDS16, and MDS45. The diagram was created using the Venn diagram web tool of the VIB and the University of Gent in Belgium (<http://bioinformatics.psb.ugent.be/webtools/Venn/>).

reference strains W83 and ATCC 33277 had 83 proteins in common, they also expressed a high number of proteins that were not shared by these two strains (60 and 41, respectively; Supplementary Figure S3B). Remarkably, the exoproteomes of the clinical isolates seemed more conserved with 115 common proteins. For the isolates 20658 and MDS16, 3 and 13 unique proteins were identified, respectively, while 60 unique proteins were identified for MDS45 (Supplementary Figure S3C).

Protein Localization Predictions Reveal Differences between the Core and Variable Exoproteomes

With the implementation of different bioinformatic tools and a manual curation based on domain identification, the subcellular localization of the identified exoproteins was predicted. The results are presented in Figure 2 and Supplementary Figure S4, showing a rather homogeneous pattern for the different isolates

with a dominant fraction of predicted outer membrane proteins and a marginal fraction of predicted inner membrane proteins among the identified exoproteins. The largest differences were observed in the relative amounts of predicted periplasmic and cytoplasmic proteins. Specifically, the predicted cytoplasmic proteins detected in the growth media of the W83, MDS16, and 20658 isolates represented ~15–20% of the whole exoproteome, while these proteins represented ~20–30% in the media of the remaining isolates. Conversely, the predicted periplasmic proteins detected for the W83, MDS16, and 20658 isolates represented ~15–20% of the whole exoproteome, while the proportion of predicted periplasmic proteins was ~10–15% for the other isolates.

In a next step, the core and variable exoproteomes of *P. gingivalis* were defined based on the presently collected data. PPAD-deficient mutants were excluded from this analysis because they were genetically engineered, whereas the PPAD gene is present in all clinical *P. gingivalis* isolates.¹⁷ The identified core exoproteome includes 64 proteins that were found for the three clinical isolates and the two reference strains. All remaining 193 proteins belong to the variable exoproteome, meaning that they were not detectable in all five of these isolates. A list of the proteins assigned to the core and variable exoproteomes is presented in Supplementary Table S1. The predicted localization of the respective proteins suggests that the core exoproteome includes a very high proportion of extracellular and outer membrane proteins (23.5 and 48.5% respectively; Figure 2A). Almost no inner membrane proteins (1.5%) and relatively low numbers of predicted cytoplasmic (12.5%) and periplasmic (14%) proteins were found in the core exoproteome. In contrast, the variable exoproteome was found to include a significantly higher proportion of predicted cytoplasmic proteins (33%) and inner membrane proteins (4%), while the proportions of predicted extracellular and outer membrane proteins was lower (14 and 33%, respectively) compared with the core exoproteome. Considering the complete set of identified extracellular proteins, the largest proportion of proteins is predicted to be outer membrane proteins (37%). About 28% of the extracellular proteins are predicted to be cytoplasmic, 16% extracellular, 15.5% periplasmic, and 3.5% inner membrane proteins (Figure 2B).

Relative Protein Abundance in *P. gingivalis* Exoproteomes

Using normalized spectral counts, a comparison of the relative abundance of identified proteins was performed. The resulting “protein secretion profiles” are presented in the heat maps in Figure 3. The data show that the 20 most abundant extracellular proteins were rather consistently present. Nevertheless, the relative amounts of these 20 exoproteins in the media of different strains, as reflected in spectral counts, differ statistically significantly in ~25% of the cases. Of note, the 20 most abundant exoproteins include the major known virulence factors of *P. gingivalis*, specifically the gingipains, fimbriae, and PPAD (Figure 3A). High differences in relative abundance were observed for the PF10365 domain protein, the major fimbrial subunit protein type-1 (FimA), a Por secretion system C-terminal sorting domain protein, and a starch-binding protein of the SusD-like family. As expected, the PPAD protein was absent from the extracellular proteomes of the two PPAD mutants. Interestingly, the presence of different fimbriae-related serotypes was reflected in the abundance of the FimA protein. FimA was not identified in the reference strain W83, the W83 PPAD mutant, and the MDS45 isolate. In contrast, FimA was

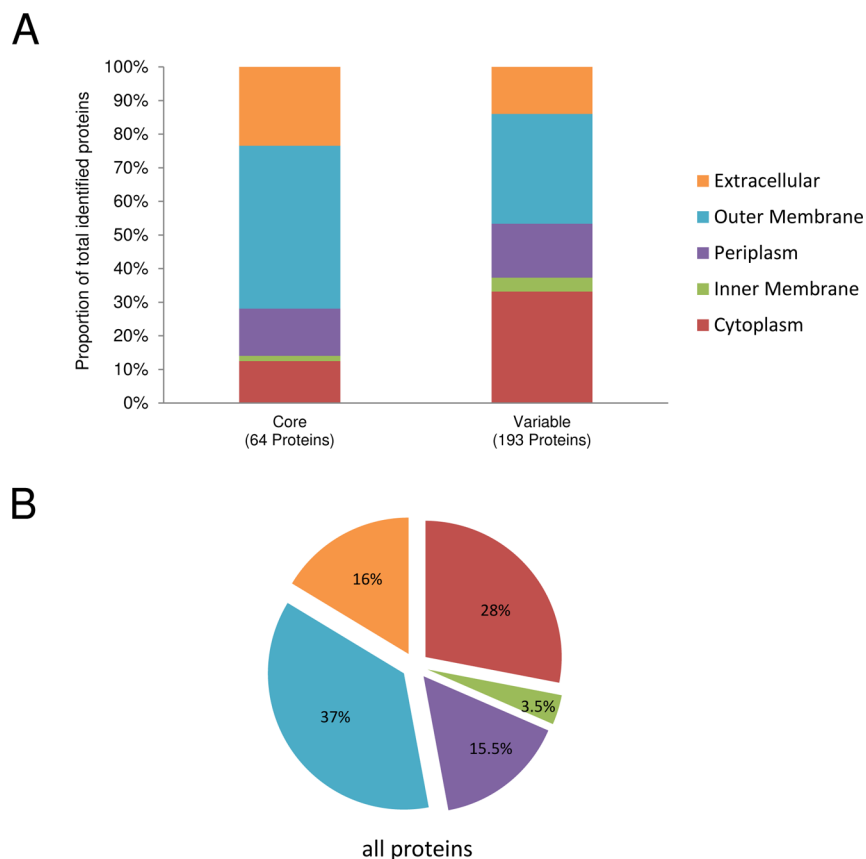


Figure 2. Localization prediction of identified proteins. The predicted subcellular or extracellular localization of the 257 identified *P. gingivalis* proteins was assessed using different algorithms as well as a manual curation based on domain identification. Percentages of proteins for each predicted localization are shown (A) for the core and variable exoproteomes and (B) for all 257 identified proteins.

found in high amounts among the extracellular proteins of the ATCC 33277 wild type and PPAD mutant and in moderate or low amounts in the MDS16 and 20658 isolates, respectively.

In contrast with the highly abundant extracellular proteins, detection of the low-abundant extracellular proteins was highly variable. This is illustrated by the heat map in Figure 3B, where the highest level of variation in detected exoproteins is observed for exoproteins of low abundance (indicated by red bars). Indeed, a statistical analysis of the differences in the amounts of the 50 least abundant exoproteins, as reflected by spectral counts, revealed that only 9% of the differences in the amounts of these exoproteins were statistically significant. This underscores the view that the detection of these low-abundance exoproteins is highly noisy. Furthermore, a clustered prediction shows that low-abundant extracellular proteins predominantly had a predicted cytoplasmic localization, while most of the highly abundant extracellular proteins were predicted to have an extracytoplasmic localization (Figure 3C).

Predicted Functions of Core and Variable Extracellular Proteins

The GO identifiers of all detected proteins were imported into REVIGO to visualize their functional background (Figure 4). Eight of the 64 identified proteins of the core exoproteome represented 7 different biological processes based on GO terms, whereas the other 56 core proteins had unknown functions (Figure 4A). The biological processes represented by core extracellular proteins were pathogenesis, cellular amino acid metabolism, anaerobic cobalamin biosynthesis, putrescine biosynthesis, protein folding, carbohydrate metabolism, and

transmembrane transport. The five most abundant proteins with known functions found in the core exoproteome were the lysine-gingipain Kgp, the two arginine-gingipains RgpA and RgpB, the agglutination protein hemagglutinin A, and the receptor antigen RagA.

Among the 193 proteins of the variable exoproteome, 72 represented 48 different biological processes based on GO terms, whereas 121 had unknown functions (Figure 4B). The most unique processes involving high numbers of the identified extracellular proteins included pathogenesis, cell redox homeostasis, protein folding, cell adhesion, iron ion transport, response to stress, and biosynthesis. The five most abundant known variable proteins were the major fimbrial subunit protein type-1 (FimA), a starch-binding protein, the receptor antigen RagB, the Mfa1 fimbriin, and the minor fimbrial component FimE.

Extracellular Citrullinome of *P. gingivalis*

To assess the possible citrullination of *P. gingivalis* proteins by PPAD, we performed a search for all arginine-containing peptides with accordant mass shifts. This resulted in a list of 25 potentially citrullinated proteins, including the gingipains, PPAD, outer membrane proteins, receptor antigens, heme-binding, and several uncharacterized proteins (Table 1). Of note, potential PPAD citrullination was only detectable in the reference strain W83 and the clinical isolate MDS45. Furthermore, previous studies suggested that proper processing of PPAD may be relevant for full enzymatic activity.^{43,44} We therefore performed a sequence coverage analysis of the extracellular PPAD (Supplementary Figure S5). This revealed

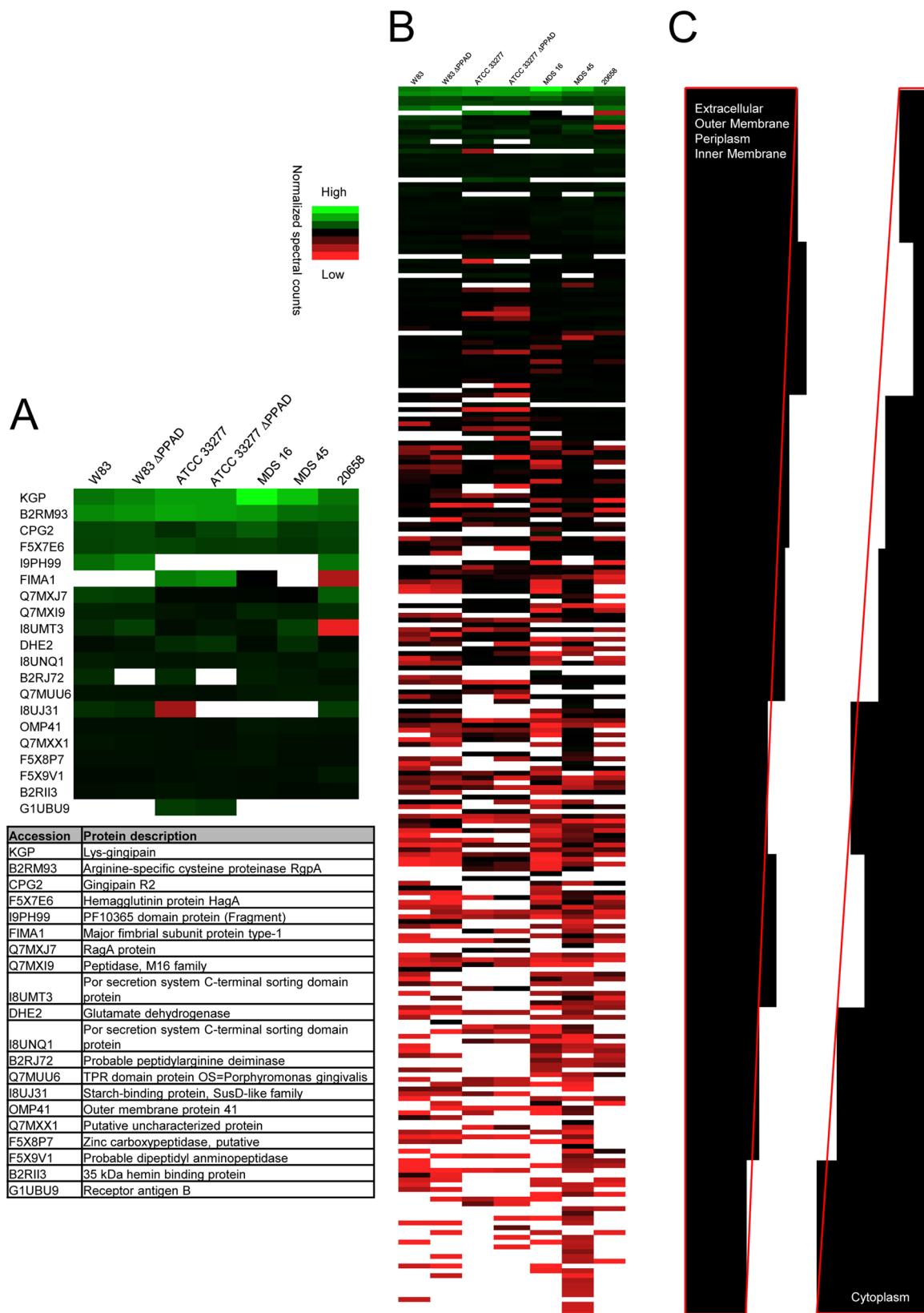


Figure 3. Exoproteome profiles of the investigated *P. gingivalis* isolates. A total number of 257 extracellular proteins was identified. Relative amounts of the identified extracellular proteins are shown based on normalized spectral counts. The *y* axis represents the proteins, and the *x* axis shows the names of the isolates. (A) 20 most abundantly secreted proteins and the respective protein descriptions. (B) Exoproteome profiles including the whole set of 257 identified extracellular proteins. (C) Clustered prediction of protein localization for the extracellular proteins displayed in panel B. The bars depict the relative abundance of proteins with predicted extracellular, outer membrane, periplasmic, or inner membrane localization (left bar) versus the relative abundance of proteins with a predicted cytoplasmic localization (right bar) per cluster of ~32 proteins.

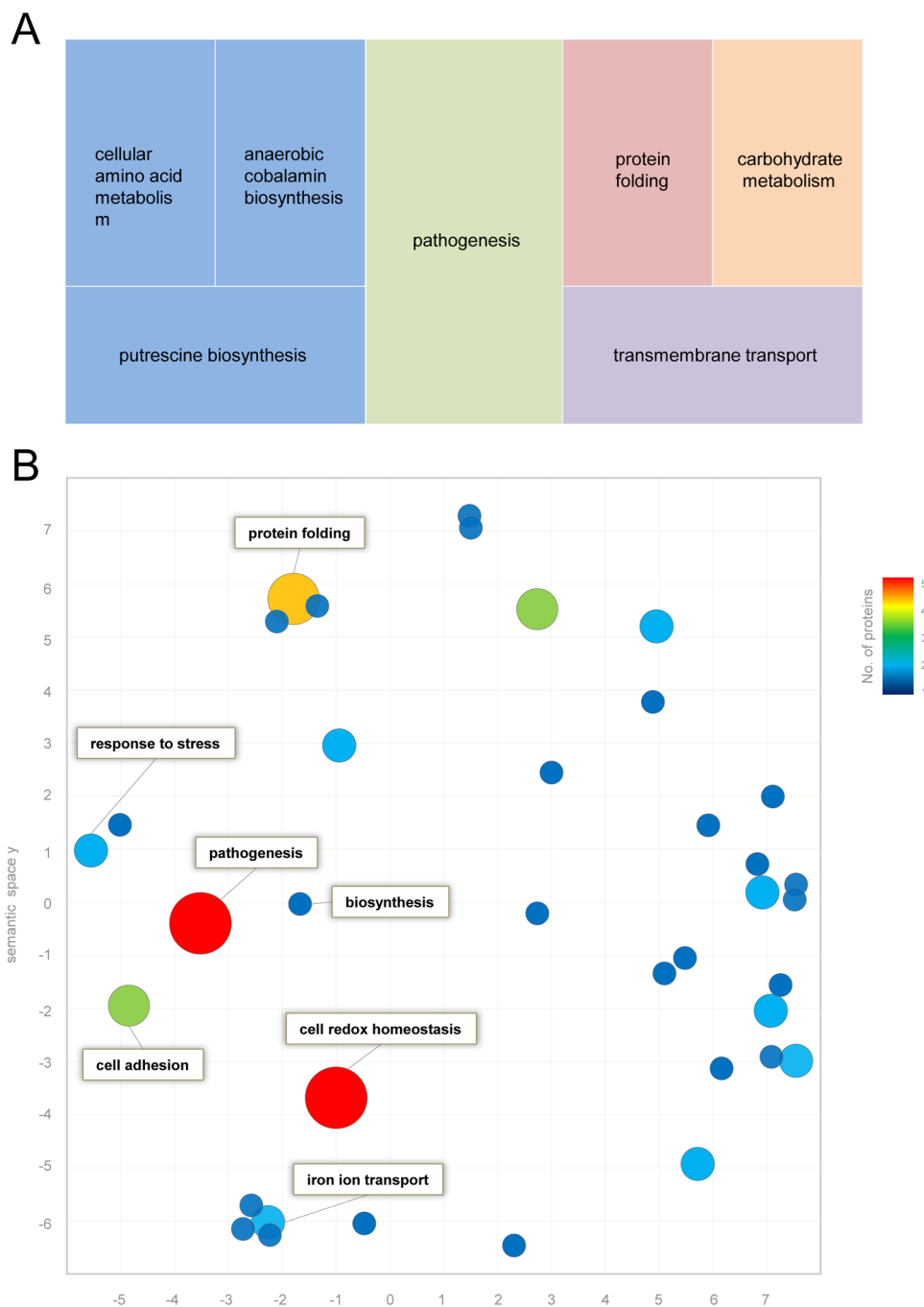


Figure 4. Functional characterization of the core and variable *P. gingivalis* exoproteome. GO terms of the present protein data set were imported into the REVIGO software to visualize their functional background. (A) Tree map of the core exoproteome. Eight of the 64 identified extracellular core proteins represented 7 different biological processes based on GO terms, whereas the other 56 core proteins had unknown functions. The colors indicate the different functional clusters, while the size of the rectangular is proportional to the number of identified proteins with the respective function. (B) Scatter plot of the variable exoproteome. Among the 193 variable extracellular proteins, 72 represented 48 different biological processes based on GO terms, whereas 121 had unknown functions. The y axis and x axis represent the semantic space. Similar or related protein functions cluster together. The size and color of the dots represent the number of proteins identified with the respective function.

the presence of two peptides from the C-terminal domain of PPAD in the W83 reference strain and the MDS45 isolate. This C-terminal domain is usually cleaved off upon secretion, suggesting the incomplete processing of PPAD in *P. gingivalis* W83 and MDS45. In contrast, no peptides from the C-terminal domain of PPAD were detectable in the reference strain ATCC 33277 and the other clinical isolates.

Notably, the above assessment of citrullination could lead to false-positive identification of citrullinated peptides because the same mass shift can also be caused by deamidation of asparagine and glutamine residues. To eliminate such potentially false-positive identifications, peptides containing asparagine or glutamine residues were excluded for a high-confidence assessment of protein citrullination. This led to the identification of six citrullinated proteins in total (Table 1),

Table 1. Overview of Citrullinated Extracellular Proteins^a

accession number	description	MW (kDa)	localization (pred.)	biological function	W83	W83 ΔPPAD	ATCC 33277	ATCC 33277 ΔPPAD	MDS 16	MDS 45	20658
B2RM93	Arginine-specific cysteine proteinase RgpA	185	Extracellular	pathogenesis	Green	Orange	Green	Orange	Green	Green	Orange
B2RLK2	Lys-gingipain	187	Extracellular	hemolysis in other organism; pathogenesis; proteolysis	Orange	Orange	Orange	Orange	Orange	Orange	Orange
F5XB86	Lysine-specific cysteine proteinase Kgp	188	Extracellular	unknown	Orange	Orange	Orange	Orange	Orange	Orange	Orange
Q7MXI9	Peptidase, M16 family	106	Cytoplasm	unknown	Orange	Orange	Orange	Orange	Orange	Orange	Orange
Q7MTV9	Putative uncharacterized protein	24	Outer Membrane	unknown	Orange	Orange	Orange	Orange	Orange	Orange	Orange
P95493	Gingipain R2	81	Extracellular	pathogenesis; proteolysis	Orange	Orange	Orange	Orange	Orange	Orange	Orange
Q9S3R9	Outer membrane protein 41	43	Outer Membrane	unknown	Orange	Orange	Orange	Orange	Orange	Orange	Orange
Q7MVM2	Putative uncharacterized protein	50	Outer Membrane	unknown	Green	Orange	Orange	Orange	Green	Green	Orange
I9P773	PF14060 domain protein	31	Periplasm	unknown	Orange	Orange	Orange	Orange	Orange	Orange	Orange
Q7MT25	Putative uncharacterized protein	27	Periplasm	unknown	Orange	Orange	Orange	Orange	Orange	Orange	Orange
Q7MXJ7	RagA protein	112	Outer Membrane	transport	Orange	Orange	Orange	Orange	Orange	Orange	Orange
F5X8P7	Zinc carboxypeptidase, putative	92	Outer Membrane	unknown	Orange	Orange	Orange	Orange	Orange	Orange	Orange
B2RIM9	Heme-binding protein FetB	33	Outer Membrane	anaerobic cobalamin biosynthetic process	Orange	Orange	Orange	Orange	Orange	Orange	Orange
B2RJ72	Probable peptidylarginine deiminase	62	Extracellular	putrescine biosynthetic process	Orange	Orange	Orange	Orange	Orange	Orange	Orange
Q7MUS3	Putative uncharacterized protein	96	Outer Membrane	transport	Orange	Orange	Orange	Orange	Orange	Orange	Orange
Q7MUA1	Putative uncharacterized protein	23	Periplasm	unknown	Orange	Orange	Orange	Orange	Orange	Green	Green
Q7MAV6	3-oxoacyl-[acyl-carrier-protein] synthase 2	45	Cytoplasm	fatty acid biosynthetic process	Orange	Orange	Orange	Orange	Orange	Orange	Orange
G1UBU7	FimA type II fimbriin	42	Outer Membrane	cell adhesion; pathogenesis	Orange	Orange	Orange	Orange	Orange	Orange	Orange
B2RHG1	Mfa1 fimbriin	61	Outer Membrane	cell-cell adhesion; pathogenesis	Orange	Orange	Orange	Orange	Orange	Green	Orange
F5XAW2	Putative lipoprotein	34	Outer Membrane	unknown	Orange	Orange	Orange	Orange	Orange	Orange	Orange
Q7MT41	LysM domain protein	56	Periplasm	unknown	Orange	Orange	Orange	Orange	Orange	Orange	Green
B2RI00	Putative uncharacterized protein	46	Outer Membrane	unknown	Orange	Orange	Orange	Orange	Orange	Orange	Orange
Q7MX91	Putative uncharacterized protein	15	Outer Membrane	unknown	Orange	Orange	Orange	Orange	Orange	Orange	Orange
B2RHG7	Receptor antigen A	115	Outer Membrane	transport	Orange	Orange	Orange	Orange	Orange	Orange	Orange
Q7MWY0	Tetratricopeptide repeat protein	52	Periplasm	unknown	Orange	Orange	Orange	Orange	Orange	Orange	Green

^aTotal of 25 proteins in the present dataset were identified as being tentatively citrullinated. Six of these proteins were identified as definitely citrullinated because the respective peptides lack asparagine and glutamine residues that could potentially be deamidated. The Table shows for each protein the Uniprot accession number, protein description, molecular weight, predicted subcellular localization, and biological function in GO terms. An orange square indicates the detection of one or more tentatively citrullinated tryptic peptides from a particular exoprotein of an indicated *P. gingivalis* isolate; a green square indicates the detection of one or more high-confidence citrullinated peptides; a white square indicates that no tentative or high-confidence citrullinated peptides were detected.

where the respective citrullinated peptides contained a C-terminal arginine residue with the exception of some citrullinated peptides from RgpA, which contained an internal citrulline (Supplementary Figure S6). Interestingly, the arginine-specific cysteine proteinase RgpA was only found to be citrullinated in the reference strains W83 and ATCC 33277 and the two RA-associated *P. gingivalis* isolates MDS16 and MDS45. Further citrullinated proteins were the Mfa1 fimbriin protein (only in MDS45) as well as four uncharacterized proteins (mainly in clinical isolates). Importantly, none of these

proteins was identified as being citrullinated in the PPAD-deficient mutants. Together, these data imply that the extracellular citrullinome of *P. gingivalis* consists of 6 to 25 proteins, including major virulence factors.

DISCUSSION

Here we present a first comparative exoproteome analysis for the oral pathogen *P. gingivalis*, including two frequently used reference strains and three clinical isolates from periodontitis patients with or without RA. Several striking observations were

made. In the first place, the two widely used reference strains show a remarkable exoproteome heterogeneity, which is only partially reflected in the exoproteomes of the three clinical isolates. Second, the vast majority of identified extracellular proteins are predicted outer membrane proteins, followed by predicted cytoplasmic proteins. The presence and abundance of proteins belonging to the latter group were found to be highly variable. Third, the functions of the identified extracellular proteins are consistent with the pathogenic lifestyle of *P. gingivalis*, which has to protect itself against severe redox stress and restricted availability of iron in the human body. Lastly, we show that 6 to 25 proteins of *P. gingivalis* belong to the PPAD-dependent extracellular citrullinome, including some of the major virulence factors of this pathogen.

The two reference strains W83 and ATCC 33277 are both widely studied and representative for the species of *P. gingivalis*. Nevertheless, it has been shown that both strains differ substantially in their pathogenicity in animal models.^{45,46} Consistent with the later findings, our present study revealed that both strains express many different proteins in their exoproteomes. This may have impact on virulence and the potential to cause disease, as was previously shown by Genco et al.⁴⁷ In fact, only about a quarter of the identified exoproteins were common to all investigated *P. gingivalis* isolates, including the two reference strains. These proteins, which make up the core exoproteome, are mainly proteins predicted to be outer membrane-associated or secreted. Well-known core exoproteins are the gingipains, agglutination proteins, and receptor antigens, which are all involved in virulence and host invasion.^{48,49} Hence these conserved exoproteins could be potential drug or vaccine targets.

Three quarters of the identified exoproteins were shown to be variable among the seven isolates and included mainly proteins involved in pathogenesis, stress responses, or cell adhesion. Fimbriae-related proteins were found to be the most abundant variable exoproteins. This is consistent with the fact that fimbriae are not found in all *P. gingivalis* isolates and that they show high genotypic variability. W83, for example, is known as an afimbriated strain because of the very low or absent expression of major fimbriae,^{50–52} which was also evidenced by the failure to detect FimA among the extracellular proteins of W83 in the present study. As a consequence, different *P. gingivalis* isolates vary in their capacity to form biofilms and to adhere to host cells.^{20,53} Furthermore, the observed differences in fimbriae detection could relate to differences in gene expression or the secretion and assembly of fimbrial subunits. Of note, most identified exoproteins (~35%) are predicted outer membrane proteins. This most likely relates to the fact that the outer membrane contains loosely anchored proteins, proteins that are liberated from the membrane by cleavage, and proteins that are released by the formation of outer membrane vesicles.^{20,54}

Intriguingly, significant differences in the total numbers of identified proteins were observed among the studied *P. gingivalis* isolates. This could relate to either differences in the activity of their secretion machinery, to differences in their susceptibility to cell lysis, or both, as previously described for other bacteria such as *Staphylococcus aureus*.⁵⁵ Most of the additionally identified proteins in the RA patient-derived *P. gingivalis* isolate MDS45 are predicted to be cytoplasmic, which suggests that this isolate may be more susceptible to cell lysis than the other studied isolates. Besides MDS45, also the reference strain ATCC 33277 and the corresponding PPAD

mutant were found to contain a relatively high proportion of predicted cytoplasmic proteins in their growth medium. Although it remains to be shown whether the predicted cytoplasmic proteins that were found extracellularly are actively secreted or released by cell lysis, these proteins may interact with the human host. For example, they could impact on the immune system by exposing new epitopes that, conceivably, might lead to the production of (auto)antibodies in a person genetically prone to develop RA. Besides that, surface-exposed cytoplasmic proteins could have particular functions related to virulence, including iron metabolism, immune evasion, and the adherence to host tissues.^{56–59} Compared with other bacteria, like *S. aureus*, Group A streptococci, and *Mycobacterium tuberculosis*,^{60,61} whose exoproteomes can contain >50% predicted cytoplasmic proteins, *P. gingivalis* seems to be a less “leaky” bacterium with a more intact membrane integrity, although this may relate to the particular growth conditions applied. It should be noted that extracellular proteases, such as the gingipains, may also impact the number of cytoplasmic proteins detected in the growth medium. As recently shown for *Bacillus subtilis*, extracellular proteases may degrade cytoplasmic proteins upon cell lysis; additionally, they may degrade particular autolysins, which would lead to reduced cell lysis.^{62–64} In both scenarios, the result is a lower amount of detectable cytoplasmic proteins in the growth medium. Consistent with this view, the *P. gingivalis* isolate MDS16, which showed the highest gingipain levels, displayed the lowest proportion of predicted cytoplasmic proteins in the growth medium.

The extracellular presence of PPAD is a common trait of all investigated wild-type *P. gingivalis* isolates¹⁷ and could be a possible connection between *P. gingivalis* and RA.^{11,13} Therefore, the extracellular citrullinome of *P. gingivalis* was analyzed. To this end, citrullinated or deamidated arginine-containing peptides were first identified. To eliminate false-positive identifications, potentially deamidated peptides were excluded from the analysis in a second step. Twenty-five proteins were found to match the first criterion, and these were shown to be mainly extracellular and membrane-associated proteins, such as proteinases, peptidases, or porins. These proteins are probably also exposed to the outer surface in an in vivo situation and might thus increase the total citrullination burden in the human host. The list of tentatively citrullinated proteins includes the PPAD of the W83 and MDS45 isolates but not the PPAD of the other investigated isolates. Intriguingly, the tentative citrullination of PPAD in the W83 and MDS45 isolates correlates with the detection of the full-length version of this enzyme and seems to be lost upon cleavage of the C-terminal domain. In this context it is noteworthy that Quirke and colleagues reported that recombinant full-length PPAD produced in *Escherichia coli* becomes autocitrullinated, while König and colleagues suggested that this autocitrullination could be an artifact of the cloning procedure that might not occur in *P. gingivalis* due to N-terminal cleavage of the protein.^{43,65} Furthermore, by excluding potentially deamidated peptides, a set of six proteins was identified as definitely citrullinated. These include the gingipain RgpA produced by the reference strains and the isolates from RA patients but not the RgpA from isolate 20658, which was obtained from a periodontitis patient. This raises the question of whether citrullination of RgpA could be a factor involved in the development of RA, especially because this citrullinated protein is secreted in high amounts. In this respect, it is noteworthy

that Kharlamova et al. recently showed that antibodies against another gingipain, RgpB, positively correlated with periodontitis, RA, and ACPA-positivity.⁶⁶ However, a possible correlation with antibodies against RgpA has not yet been assessed and should be subject of future investigations. Besides RgpA, four unknown proteins and the fimbrial protein Mfa1 were found to be citrullinated. Citrullination of surface structures, such as the fimbriae, could also represent a potential trigger of ACPA formation because these structures are among the first to make contact with immune cells of the host (e.g., macrophages or dendritic cells).⁶⁷ Conceivably, this could trigger an auto-immune response against these and other citrullinated proteins in the host.

Investigation of the characteristics of the identified citrullinated peptides revealed that most of these peptides contained a C-terminal citrulline, except for some peptides of RgpA that contained an internal citrulline (Figure S6). A recent study by Bennike et al. showed that trypsin is unable to cleave C-terminally of citrulline residues, which can be used to verify the citrullination of particular peptides through a lack of trypsin-mediated cleavage of these peptides.⁶⁸ Furthermore, Bennike et al. concluded that manual curation of tentative citrullinated peptides is essential. Another study by Wegner et al. indicated that PPAD is only able to citrullinate C-terminal arginine residues, which implies that proteins first need to be cleaved by the arginine-specific gingipains RgpA or RgpB to expose a C-terminal arginine that can then serve as substrate for PPAD.¹⁸ Indeed, the peptides presently identified as being citrullinated mostly contained C-terminal citrulline residues, and, in fact, many of them represented the C-termini of the respective proteins (Figure S6). Hence, these peptides were probably citrullinated by PPAD while being part of the native protein. Other identified peptides with a C-terminal citrulline, which are located within the polypeptide chain of particular proteins, were probably first processed by RgpA or RgpB and then citrullinated by PPAD, as was proposed by Wegner et al. The few peptides with tentative internal citrulline residues may either represent misannotations or could reflect the presumably infrequent citrullination of internal arginine residues by PPAD.

CONCLUSIONS

The present study provides a broad overview on the heterogeneity of the extracellular proteome and citrullinome of the important oral pathogen *P. gingivalis*. Main differences were found in the extracellular presence of low-abundant predicted cytoplasmic proteins and in the citrullination status of particular proteins, while the presence of most of the known highly abundant virulence factors was demonstrated for all investigated isolates. With respect to the development of RA, our observations focus special attention on the 6 to 25 proteins that were found to be (potentially) citrullinated, especially the gingipain RgpA. Accordingly, our future studies will include larger collections of *P. gingivalis* isolates, and they will focus attention on possible correlations between particular *P. gingivalis* exoproteome or citrullinome profiles and the inflammatory diseases periodontitis and RA.

ASSOCIATED CONTENT

Supporting Information

The Supporting Information is available free of charge on the ACS Publications website at DOI: 10.1021/acs.jproteome.6b00634.

Table S1. Overview of identified extracellular proteins in the present study with peptide and spectral count information. (XLSX)

Figure S1. Growth curves of *P. gingivalis* in liquid culture.

Figure S2. LDS-PAGE of exoproteome samples

Figure S3. Numbers of proteins in the exoproteomes of the *P. gingivalis* isolates.

Figure S4. Localization prediction of identified proteins per isolate.

Figure S5. Sequence coverage and modifications of PPAD. (PDF)

Figure S6. Spectra and fragmentation tables of citrullinated proteins. (PDF)

Supplementary FASTA file. Nonredundant *P. gingivalis* database concatenated with common laboratory contaminants and a target-pseudoreversed decoy database. (ZIP)

AUTHOR INFORMATION

Corresponding Author

*E-mail: j.m.van.dijl01@umcg.nl. Phone: +31-50-3615187.

Author Contributions

[†]T.S. and C.G. contributed equally.

Notes

The authors declare the following competing financial interest(s): Prof. Dr. Arie Jan van Winkelhoff is co-owner of Laboral Diagnostics, a service in the field of clinical microbiology for dental professionals. The other authors declare no conflicts of interest.

ACKNOWLEDGMENTS

We thank Natalia Wegner and Ky-Anh Nguyen for kindly providing the PPAD-deficient mutants of *P. gingivalis* ATCC 33277 and W83. This work was supported by the Graduate School of Medical Sciences of the University of Groningen (T.S., C.G., J.M.v.D.), and the Center for Dentistry and Oral Hygiene of the University Medical Center Groningen (G.G., M.d.S., A.J.v.W.).

ABBREVIATIONS

ACPA, anticitrullinated protein antibodies; BA2, blood agar base no. 2; BHI, brain heart infusion; BSL-2, biosafety level 2; CID, collision-induced dissociation; ESI, electrospray ionization; GO, gene ontology; IAA, iodoacetamide; LC, liquid chromatography; LDS, lithium dodecyl sulfate; LPS, lipopolysaccharide; MALDI-TOF, matrix-assisted laser desorption/ionization-time-of-flight; MS, mass spectrometry; OD, optical density at 600 nm; PAD, peptidylarginine deiminase; PPAD, *Porphyromonas gingivalis* peptidylarginine deiminase; RA, rheumatoid arthritis; TCA, trichloroacetic acid; TFA, trifluoroacetic acid

REFERENCES

- (1) Jansson, H. Studies on periodontitis and analyses of individuals at risk for periodontal diseases. *Swed. Dent. J. Suppl.* **2006**, No. No. 180, 5–49.
- (2) Berthelot, J.-M.; Le Goff, B. Rheumatoid arthritis and periodontal disease. *Jt., Bone, Spine* **2010**, *77* (6), 537–41.
- (3) Yilmaz, O. The chronicles of *Porphyromonas gingivalis*: the microbium, the human oral epithelium and their interplay. *Microbiology (London, U. K.)* **2008**, *154* (10), 2897–903.
- (4) Bostanci, N.; Belibasakis, G. N. *Porphyromonas gingivalis*: an invasive and evasive opportunistic oral pathogen. *FEMS Microbiol. Lett.* **2012**, *333* (1), 1–9.

- (5) Griffen, A. L.; Becker, M. R.; Lyons, S. R.; Moeschberger, M. L.; Leys, E. J. Prevalence of Porphyromonas gingivalis and periodontal health status. *J. Clin. Microbiol.* **1998**, *36* (11), 3239–42.
- (6) van Winkelhoff, A. J.; Loos, B. G.; van der Reijden, W. A.; van der Velden, U. Porphyromonas gingivalis, Bacteroides forsythus and other putative periodontal pathogens in subjects with and without periodontal destruction. *J. Clin. Periodontol.* **2002**, *29* (11), 1023–8.
- (7) Lundberg, K.; Wegner, N.; Yucel-Lindberg, T.; Venables, P. J. Periodontitis in RA-the citrullinated enolase connection. *Nat. Rev. Rheumatol.* **2010**, *6* (12), 727–30.
- (8) Hajishengallis, G. Periodontitis: from microbial immune subversion to systemic inflammation. *Nat. Rev. Immunol.* **2014**, *15* (1), 30–44.
- (9) de Smit, M.; Westra, J.; Vissink, A.; Doornbos-van der Meer, B.; Brouwer, E.; van Winkelhoff, A. J. Periodontitis in established rheumatoid arthritis patients: a cross-sectional clinical, microbiological and serological study. *Arthritis research & therapy* **2012**, *14* (5), R222.
- (10) Routsias, J. G.; Goules, J. D.; Goules, A.; Charalampakis, G.; Pikazis, D. Autopathogenic correlation of periodontitis and rheumatoid arthritis. *Rheumatology (Oxford, U. K.)* **2011**, *50* (7), 1189–93.
- (11) de Smit, M. J.; Brouwer, E.; Vissink, A.; van Winkelhoff, A. J. Rheumatoid arthritis and periodontitis; a possible link via citrullination. *Anaerobe* **2011**, *17* (4), 196–200.
- (12) van der Helm-van Mil, A. H. M.; Verpoort, K. N.; Breedveld, F. C.; Toes, R. E. M.; Huizinga, T. W. J. Antibodies to citrullinated proteins and differences in clinical progression of rheumatoid arthritis. *Arthritis research & therapy* **2005**, *7*, R949–58.
- (13) Mangat, P.; Wegner, N.; Venables, P. J.; Potempa, J. Bacterial and human peptidylarginine deiminases: targets for inhibiting the autoimmune response in rheumatoid arthritis? *Arthritis research & therapy* **2010**, *12* (3), 209.
- (14) Mohamed, B. M.; Verma, N. K.; Davies, A. M.; McGowan, A.; Crosbie-Staunton, K.; Prina-Mello, A.; Kelleher, D.; Botting, C. H.; Causey, C. P.; Thompson, P. R.; et al. Citrullination of proteins: a common post-translational modification pathway induced by different nanoparticles in vitro and in vivo. *Nanomedicine (London, U. K.)* **2012**, *7* (8), 1181–95.
- (15) Thompson, P. R.; Fast, W. Histone citrullination by protein arginine deiminase: is arginine methylation a green light or a roadblock? *ACS Chem. Biol.* **2006**, *1* (7), 433–41.
- (16) Baka, Z.; György, B.; Géher, P.; Buzás, E. I.; Falus, A.; Nagy, G. Citrullination under physiological and pathological conditions. *Jt, Bone, Spine* **2012**, *79* (5), 431–6.
- (17) Gabarrini, G.; de Smit, M.; Westra, J.; Brouwer, E.; Vissink, A.; Zhou, K.; Rossen, J. W. A.; Stoberneck, T.; van Dijk, J. M.; van Winkelhoff, A. J. The peptidylarginine deiminase gene is a conserved feature of Porphyromonas gingivalis. *Sci. Rep.* **2015**, *5*, 13936.
- (18) Wegner, N.; Wait, R.; Sroka, A.; Eick, S.; Nguyen, K.-A.; Lundberg, K.; Kinloch, A.; Culshaw, S.; Potempa, J.; Venables, P. J. Peptidylarginine deiminase from Porphyromonas gingivalis citrullinates human fibrinogen and α -enolase: implications for autoimmunity in rheumatoid arthritis. *Arthritis Rheum.* **2010**, *62* (9), 2662–72.
- (19) McGraw, W. T.; Potempa, J.; Farley, D.; Travis, J. Purification, characterization, and sequence analysis of a potential virulence factor from Porphyromonas gingivalis, peptidylarginine deiminase. *Infect. Immun.* **1999**, *67* (7), 3248–56.
- (20) Yoshimura, F.; Murakami, Y.; Nishikawa, K.; Hasegawa, Y.; Kawaminami, S. Surface components of Porphyromonas gingivalis. *J. Periodontal Res.* **2009**, *44* (1), 1–12.
- (21) Yoshimura, M.; Ohara, N.; Kondo, Y.; Shoji, M.; Okano, S.; Nakano, Y.; Abiko, Y.; Nakayama, K. Proteome analysis of Porphyromonas gingivalis cells placed in a subcutaneous chamber of mice. *Oral Microbiol. Immunol.* **2008**, *23* (5), 413–8.
- (22) Osbourne, D.; Aruni, A. W.; Dou, Y.; Perry, C.; Boskovic, D. S.; Roy, F.; Fletcher, H. M. VImA-dependent modulation of the secretome in Porphyromonas gingivalis. *Mol. Oral Microbiol.* **2012**, *27* (6), 420–35.
- (23) Hendrickson, E. L.; Xia, Q.; Wang, T.; Lamont, R. J.; Hackett, M. Pathway analysis for intracellular Porphyromonas gingivalis using a strain ATCC 33277 specific database. *BMC Microbiol.* **2009**, *9*, 185.
- (24) Zhang, Y.; Wang, T.; Chen, W.; Yilmaz, O.; Park, Y.; Jung, I.-Y.; Hackett, M.; Lamont, R. J. Differential protein expression by Porphyromonas gingivalis in response to secreted epithelial cell components. *Proteomics* **2005**, *5* (1), 198–211.
- (25) Cogo, K.; de Andrade, A.; Labate, C. A.; Bergamaschi, C. C.; Berto, L. A.; Franco, G. C. N.; Gonçalves, R. B.; Groppo, F. C. Proteomic analysis of Porphyromonas gingivalis exposed to nicotine and cotinine. *J. Periodontal Res.* **2012**, *47* (6), 766–75.
- (26) Xia, Q.; Wang, T.; Taub, F.; Park, Y.; Capestany, C. A.; Lamont, R. J.; Hackett, M. Quantitative proteomics of intracellular Porphyromonas gingivalis. *Proteomics* **2007**, *7* (23), 4323–37.
- (27) Maeda, K.; Nagata, H.; Ojima, M.; Amano, A. Proteomic and Transcriptional Analysis of Interaction between Oral Microbiota Porphyromonas gingivalis and Streptococcus oralis. *J. Proteome Res.* **2015**, *14*, 82–94.
- (28) Veloo, A. C. M.; Elgersma, P. E.; Friedrich, A. W.; Nagy, E.; van Winkelhoff, A. J. The influence of incubation time, sample preparation and exposure to oxygen on the quality of the MALDI-TOF MS spectrum of anaerobic bacteria. *Clin. Microbiol. Infect.* **2014**, *20* (12), O1091–7.
- (29) Dreisbach, A.; Hempel, K.; Buist, G.; Hecker, M.; Becher, D.; van Dijk, J. M. Profiling the surfacome of Staphylococcus aureus. *Proteomics* **2010**, *10* (17), 3082–96.
- (30) Bonn, F.; Bartel, J.; Büttner, K.; Hecker, M.; Otto, A.; Becher, D. Picking vanished proteins from the void: how to collect and ship/share extremely dilute proteins in a reproducible and highly efficient manner. *Anal. Chem.* **2014**, *86* (15), 7421–7.
- (31) Vizcaino, J. A.; Deutsch, E. W.; Wang, R.; Csordas, A.; Reisinger, F.; Rios, D.; Dianes, J. A.; Sun, Z.; Farrar, T.; Bandeira, N.; et al. ProteomeXchange provides globally coordinated proteomics data submission and dissemination. *Nat. Biotechnol.* **2014**, *32* (3), 223–226.
- (32) Juncker, A. S.; Willenbrock, H.; von Heijne, G.; Brunak, S.; Nielsen, H.; Krogh, A. Prediction of lipoprotein signal peptides in Gram-negative bacteria. *Protein Sci.* **2003**, *12* (8), 1652.
- (33) Berven, F. S.; Karlsen, O. A.; Straume, A. H.; Flikka, K.; Murrell, J. C.; Fjellbirkeland, A.; Lillehaug, J. R.; Eidhammer, I.; Jensen, H. B. Analysing the outer membrane subproteome of Methylococcus capsulatus (Bath) using proteomics and novel biocomputing tools. *Arch. Microbiol.* **2006**, *184* (6), 362–77.
- (34) Sonnhammer, E. L.; Heijne, von, G.; Krogh, A. A hidden Markov model for predicting transmembrane helices in protein sequences. *Proc. - Int. Conf. Intell. Syst. Mol. Biol.* **1998**, *6*, 175–82.
- (35) Krogh, A.; Larsson, B.; von Heijne, G.; Sonnhammer, E. L. Predicting transmembrane protein topology with a hidden Markov model: application to complete genomes. *J. Mol. Biol.* **2001**, *305* (3), 567–80.
- (36) Käll, L.; Krogh, A.; Sonnhammer, E. L. L. A combined transmembrane topology and signal peptide prediction method. *J. Mol. Biol.* **2004**, *338* (5), 1027–36.
- (37) Petersen, T. N.; Brunak, S.; von Heijne, G.; Nielsen, H. SignalP 4.0: discriminating signal peptides from transmembrane regions. *Nat. Methods* **2011**, *8* (10), 785–6.
- (38) Hiller, K.; Grote, A.; Scheer, M.; Münch, R.; Jahn, D. PrediSi: prediction of signal peptides and their cleavage positions. *Nucleic Acids Res.* **2004**, *32* (Web Server), W375–9.
- (39) Bendtsen, J. D.; Kiemer, L.; Fausbøll, A.; Brunak, S. Non-classical protein secretion in bacteria. *BMC Microbiol.* **2005**, *5*, 58.
- (40) Yu, N. Y.; Wagner, J. R.; Laird, M. R.; Melli, G.; Rey, S.; Lo, R.; Dao, P.; Sahinalp, S. C.; Ester, M.; Foster, L. J.; et al. PSORTb 3.0: improved protein subcellular localization prediction with refined localization subcategories and predictive capabilities for all prokaryotes. *Bioinformatics* **2010**, *26* (13), 1608–15.
- (41) Paramasivam, N.; Linke, D. ClubSub-P: Cluster-Based Subcellular Localization Prediction for Gram-Negative Bacteria and Archaea. *Front. Microbiol.* **2011**, *2*, 218.

- (42) Supek, F.; Bošnjak, M.; Škunca, N.; Šmuc, T. REVIGO summarizes and visualizes long lists of gene ontology terms. *PLoS One* **2011**, *6* (7), e21800.
- (43) Konig, M. F.; Paracha, A. S.; Moni, M.; Bingham, C. O.; Andrade, F. Defining the role of *Porphyromonas gingivalis* peptidylarginine deiminase (PPAD) in rheumatoid arthritis through the study of PPAD biology. *Ann. Rheum. Dis.* **2015**, *74*, 2054–61.
- (44) Rodríguez, S. B.; Stitt, B. L.; Ash, D. E. Expression of peptidylarginine deiminase from *Porphyromonas gingivalis* in *Escherichia coli*: enzyme purification and characterization. *Arch. Biochem. Biophys.* **2009**, *488* (1), 14–22.
- (45) Neiders, M. E.; Chen, P. B.; Suido, H.; Reynolds, H. S.; Zambon, J. J.; Shlossman, M.; Genco, R. J. Heterogeneity of virulence among strains of *Bacteroides gingivalis*. *J. Periodontol. Res.* **1989**, *24* (3), 192–198.
- (46) Igboin, C. O.; Moeschberger, M. L.; Griffen, A. L.; Leys, E. J. *Porphyromonas gingivalis* virulence in a *Drosophila melanogaster* model. *Infection and immunity* **2011**, *79* (1), 439–448.
- (47) Genco, C. A.; Cutler, C. W.; Kapczynski, D.; Maloney, K.; Arnold, R. R. A novel mouse model to study the virulence of and host response to *Porphyromonas (Bacteroides) gingivalis*. *Infect. Immun.* **1991**, *59*, 1255–1263.
- (48) Chen, T.; Nakayama, K.; Belliveau, L.; Duncan, M. J. *Porphyromonas gingivalis* gingipains and adhesion to epithelial cells. *Infection and immunity* **2001**, *69* (5), 3048–3056.
- (49) Curtis, M. A.; Opoku, J. A.; Rangarajan, M.; Gallagher, A.; Sterne, J. A. C.; Reid, C. R.; Evans, H. E. A.; Samuelsson, B. Attenuation of the virulence of *Porphyromonas gingivalis* by using a specific synthetic Kgp protease inhibitor. *Infection and immunity* **2002**, *70* (12), 6968–6975.
- (50) Zheng, C.; Wu, J.; Xie, H. Differential expression and adherence of *Porphyromonas gingivalis* FimA genotypes. *Mol. Oral Microbiol.* **2011**, *26* (6), 388–395.
- (51) Hayashi, J.; Nishikawa, K.; Hirano, R.; Noguchi, T.; Yoshimura, F. Identification of a two-component signal transduction system involved in fimbriation of *Porphyromonas gingivalis*. *Microbiol. Immunol.* **2000**, *44* (4), 279–282.
- (52) Nishikawa, K.; Duncan, M. J. Histidine kinase-mediated production and autoassembly of *Porphyromonas gingivalis* fimbriae. *J. Bacteriol.* **2010**, *192* (7), 1975–1987.
- (53) Barbosa, G. M.; Colombo, A. V.; Rodrigues, P. H.; Simionato, M. R. L. Intraspecies Variability Affects Heterotypic Biofilms of *Porphyromonas gingivalis* and *Prevotella intermedia*: Evidences of Strain-Dependence Biofilm Modulation by Physical Contact and by Released Soluble Factors. *PLoS One* **2015**, *10* (9), e0138687.
- (54) Veith, P. D.; Chen, Y.-Y.; Gorasia, D. G.; Chen, D.; Glew, M. D.; O'Brien-Simpson, N. M.; Cecil, J. D.; Holden, J. A.; Reynolds, E. C. *Porphyromonas gingivalis* outer membrane vesicles exclusively contain outer membrane and periplasmic proteins and carry a cargo enriched with virulence factors. *J. Proteome Res.* **2014**, *13* (5), 2420–32.
- (55) Matsuda, K.; Nakamura, K.; Adachi, Y.; Inoue, M.; Kawakami, M. Autolysis of methicillin-resistant *Staphylococcus aureus* is involved in synergism between imipenem and cefotiam. *Antimicrob. Agents Chemother.* **1995**, *39* (12), 2631–2634.
- (56) Mohan, S.; Hertweck, C.; Dudda, A.; Hammerschmidt, S.; Skerka, C.; Hallström, T.; Zipfel, P. F. Tuf of *Streptococcus pneumoniae* is a surface displayed human complement regulator binding protein. *Mol. Immunol.* **2014**, *62* (1), 249–264.
- (57) Boradia, V. M.; Raje, M.; Raje, C. I. Protein moonlighting in iron metabolism: glyceraldehyde-3-phosphate dehydrogenase (GAPDH). *Biochem. Soc. Trans.* **2014**, *42* (6), 1796–1801.
- (58) Dreisbach, A.; van Dijk, J. M.; Buist, G. The cell surface proteome of *Staphylococcus aureus*. *Proteomics* **2011**, *11* (15), 3154–3168.
- (59) Henderson, B. An overview of protein moonlighting in bacterial infection. *Biochem. Soc. Trans.* **2014**, *42* (6), 1720–1727.
- (60) Hempel, K.; Herbst, F.-A.; Moche, M.; Hecker, M.; Becher, D. Quantitative proteomic view on secreted, cell surface-associated, and cytoplasmic proteins of the methicillin-resistant human pathogen *Staphylococcus aureus* under iron-limited conditions. *J. Proteome Res.* **2011**, *10* (4), 1657–66.
- (61) Tjalsma, H.; Antelmann, H.; Jongbloed, J. D. H.; Braun, P. G.; Darmon, E.; Dorenbos, R.; Dubois, J.-Y. F.; Westers, H.; Zanen, G.; Quax, W. J.; et al. Proteomics of protein secretion by *Bacillus subtilis*: separating the “secrets” of the secretome. *Microbiol. Mol. Biol. Rev.* **2004**, *68* (2), 207–233.
- (62) Antelmann, H.; Tjalsma, H.; Voigt, B.; Ohlmeier, S.; Bron, S.; van Dijk, J. M.; Hecker, M. A proteomic view on genome-based signal peptide predictions. *Genome Res.* **2001**, *11* (9), 1484–1502.
- (63) Krishnappa, L.; Monteferrante, C. G.; Neef, J.; Dreisbach, A.; van Dijk, J. M. Degradation of extracytoplasmic catalysts for protein folding in *Bacillus subtilis*. *Appl. Environ. Microbiol.* **2014**, *80* (4), 1463–1468.
- (64) Krishnappa, L.; Dreisbach, A.; Otto, A.; Goosens, V. J.; Cranenburgh, R. M.; Harwood, C. R.; Becher, D.; van Dijk, J. M. Extracytoplasmic proteases determining the cleavage and release of secreted proteins, lipoproteins, and membrane proteins in *Bacillus subtilis*. *J. Proteome Res.* **2013**, *12* (9), 4101–4110.
- (65) Quirke, A.-M.; Lugli, E. B.; Wegner, N.; Hamilton, B. C.; Charles, P.; Chowdhury, M.; Ytterberg, A. J.; Zubarev, R. A.; Potempa, J.; Culshaw, S.; et al. Heightened immune response to autocitrullinated *Porphyromonas gingivalis* peptidylarginine deiminase: a potential mechanism for breaching immunologic tolerance in rheumatoid arthritis. *Ann. Rheum. Dis.* **2014**, *73* (1), 263–9.
- (66) Kharlamova, N.; Jiang, X.; Sherina, N.; Potempa, B.; Israelsson, L.; Quirke, A.-M.; Eriksson, K.; Yucel-Lindberg, T.; Venables, P. J.; Potempa, J.; et al. Antibodies to *Porphyromonas gingivalis* indicate interaction between oral infection, smoking and risk genes in rheumatoid arthritis etiology. *Arthritis Rheumatol.* **2016**, *68*, 604–13.
- (67) Takeshita, A.; Murakami, Y.; Yamashita, Y.; Ishida, M.; Fujisawa, S.; Kitano, S.; Hanazawa, S. *Porphyromonas gingivalis* fimbriae use beta2 integrin (CD11/CD18) on mouse peritoneal macrophages as a cellular receptor, and the CD18 beta chain plays a functional role in fimbrial signaling. *Infect. Immun.* **1998**, *66*, 4056–4060.
- (68) Bennike, T.; Lauridsen, K. B.; Olesen, M. K.; Andersen, V.; Birkelund, S.; Stensballe, A. Optimizing the Identification of Citrullinated Peptides by Mass Spectrometry: Utilizing the Inability of Trypsin to Cleave after Citrullinated Amino Acids. *J. Proteomics Bioinf.* **2013**, *6* (12), 288–295.